On the Extraordinary Optical Transmission in parallel plate waveguides for non-TEM modes

Miguel Camacho,[1,*] Rafael R. Boix,[2] Francisco Medina,[2] Alastair P. Hibbins,[1] and J. Roy Sambles[1]

[1] *Electromagnetic and Acoustic Materials Group, Department of Physics and Astronomy, University of Exeter, Stocker Road, Exeter EX4 4QL, United Kingdom*
[2] *Department of Electronics and Electromagnetism, College of Physics, University of Seville, Avda. Reina Mercedes s/n, Seville, Spain*
[*] *mc586@exeter.ac.uk*

Abstract: Extraordinary transmission has been recently measured in a parallel plate waveguide (PPWG) through a metal strip with a patterned 1-D periodic array of circular holes, the metal strip being embedded inside the PPWG. Wood's anomaly and the extraordinary transmission peak (EOT) were detected for transverse electric (TE) mode excitation at frequencies higher than those found for TEM mode excitation. In this paper we provide an explanation for this frequency shift by decomposing the problem of a TE mode impinging on the 1-D array of holes into two problems of plane waves impinging obliquely on 2-D periodic arrays of holes. By then solving the integral equation for the electric field on the surface of the holes, the origin of the frequency shift is proved both mathematically and physically in terms of the symmetries present in the system.

OCIS codes: (230.7370) Waveguides; (050.1755) Computational electromagnetic methods, (260.2110) Electromagnetic optics.

References and links

1. T. W. Ebbesen, H. J. Lezec, H. F. Ghaemi, T. Thio, and P. A. Wolff, "Extraordinary optical transmission through sub-wavelength hole arrays," Nature **391**, 667–669 (1998).
2. H. A. Bethe, "Theory of diffraction by small holes," Phys. Rev. **66**, 163–182 (1944).
3. H. F. Ghaemi, T. Thio, D. E. Grupp, T. W. Ebbesen, and H. J. Lezec, "Surface plasmons enhance optical transmission through subwavelength holes," Phys. Rev. B **58**, 6779–6782 (1998).
4. M. Beruete, M. Sorolla, I. Campillo, J. S. Dolado, L. Martín-Moreno, J. Bravo-Abad, and F. J. García-Vidal, "Enhanced millimeter-wave transmission through subwavelength hole arrays," Opt. Lett. **29**, 2500 (2004).
5. J. B. Pendry, L. Martín-Moreno, and F. J. Garcia-Vidal, "Mimicking surface plasmons with structured surfaces." Science **305**, 847–8 (2004).
6. F. J. García De Abajo, and J. J. Sáenz, "Electromagnetic surface modes in structured perfect-conductor surfaces." Phys. Rev. Lett., **95** 233901 (2005),
7. F. J. Garcia-Vidal, L. Martin-Moreno, T. W. Ebbesen, and L. Kuipers, "Light passing through subwavelength apertures," Rev. Mod. Phys. **82**, 729–787 (2010).
8. C. Genet and T. W. Ebbesen, "Light in tiny holes," Nature **445**, 39–46 (2007).
9. F. J. Garcia De Abajo, "Colloquium: Light scattering by particle and hole arrays," Rev. Mod. Phys. **79**, 1267–1290 (2007).
10. J. Bravo-Abad, A. I. Fernández-Domínguez, F. J. García-Vidal, and L. Martín-Moreno, "Theory of extraordinary transmission of light through quasiperiodic arrays of subwavelength holes," Phys. Rev. Lett. **99**, 203905 (2007).
11. M. Camacho, R. R. Boix, and F. Medina, "Comparative study between resonant transmission and extraordinary transmission in truncated periodic arrays of slots," in "2017 IEEE MTT-S International Conference on Numerical Electromagnetic and Multiphysics Modeling and Optimization for RF, Microwave, and Terahertz Applications (NEMO)," (IEEE, 2017), pp. 257–259.
12. Y. Pang, A. Hone, P. So, and R. Gordon, "Total optical transmission through a small hole in a metal waveguide screen," Opt. Express **17**, 4433–4441 (2009).
13. F. Medina, J. A. Ruiz-Cruz, F. Mesa, J. M. Rebollar, J. R. Montejo-Garai, and R. Marqués, "Experimental verification of extraordinary transmission without surface plasmons," Appl. Phys. Lett. **95**, 071102 (2009).
14. F. Medina, F. Mesa, and R. Marqués, "Extraordinary transmission through arrays of electrically small holes from a circuit theory perspective," IEEE Trans. Microw. Theory Techn. **56**, 3108–3120 (2008).
15. K. S. Reichel, P. Y. Lu, S. Backus, R. Mendis, and D. M. Mittleman, "Extraordinary optical transmission inside a waveguide: spatial mode dependence," Opt. Express **24**, 28221 (2016).

16. D. M. Pozar, *Microwave Engineering* (John Wiley & Sons Inc, 2005).
17. M. Camacho, R. R. Boix, and F. Medina, "Computationally efficient analysis of extraordinary optical transmission through infinite and truncated subwavelength hole arrays," Phys. Rev. E **93**, 063312 (2016).
18. M. Camacho, R. R. Boix, F. Medina, A. P. Hibbins, and J. R. Sambles, "Theoretical and experimental exploration of finite sample size effects on the propagation of surface waves supported by slot arrays," Phys. Rev. B **95**, 245425 (2017).
19. R. F. Harrington, *Field Computation by Moment Methods* (Wiley-IEEE, 1993).

1. Introduction

With the experimental discovery of extraordinary optical transmission (EOT) in the late nineteen nineties [1], it was unveiled that the transmission through small holes could be accomplished by taking advantage of periodicity, largely overcoming the predictions of Bethe's single aperture theory [2]. It was found that an enhanced transmission peak was always present at a frequency lower than that of the first onset of diffraction, even when the intrinsic resonance of the hole was well above the latter. In the optical regime, this was explained through the coupling of the free space radiation to bound modes commonly known as surface plasmon polaritons (SPPs) [3]. The finding of enhanced transmission at frequencies at which metals do not support SPPs, such as microwaves [4], made it clear that genuine SPPs were not essential to explain EOT. The EOT theory was later unified across a large range of frequencies thanks to the existence of surface modes supported by periodic arrays of holes at microwave frequencies, which were shown in some cases to behave in a similar dispersive manner to the optical SPPs [5, 6]. A large body of work has been undertaken by both the optics and microwave engineering communities on this topic, collected into extensive review articles [7–9] and it still remains important due to the rich physics behind it [10, 11].

Although most of the studies of the transmission through small apertures have been based on free-space wave propagation, the EOT phenomenon is also found in the transmission through metallic waveguide diaphragms near the cut-off of higher order waveguide modes, which play the role of the onset of diffracted modes in periodic structures [12, 13]. Moreover, the use of transmission line theory to explain the EOT as an impedance matching problem is based on the transverse electromagnetic (TEM) mode supported by a parallel plate waveguide (PPWG) [14].

Only recently has the EOT effect been studied for transmission through a 1-D periodic array of circular holes embedded in a PPWG by Reichel *et al.* [15]. In particular, these researchers measured and computed the transmission coefficient when the array was excited both by the TEM mode and by the PPWG TE_1 mode. They found that the EOT peak appears at higher frequencies in the latter case than in the former case.

In this paper we present an approach to understand the origin of the EOT peak frequency shift in PPWG under TE_1 mode excitation. This theory is based on the decomposition of the problem into two problems of EOT through a 2-D periodic array of symmetric holes under oblique plane wave excitation. These EOT problems are in turn accurately analyzed by solving an integral equation involving a periodic Green's function. The steps followed in the solution of the integral equation provide a way to predict the appearance of Wood's anomalies and the associated extraordinary transmission through both the 2-D array of holes and the equivalent 1-D array of holes in PPWG under TE_1 mode excitation. Our approach provides new physical insight into the origin of Wood's anomalies and proposes a highly efficient analysis tool for the numerical study of structures supporting EOT phenomena. It only requires the solution of a small system of equations to obtain accurate results as opposite to other numerical methods such as coupled-mode method (also known as mode-matching). And this is because it adequately accounts for the singular behavior of the field quantities at the edges of the metal screen holes. This singular behavior cannot be handled by the expansion modes used in the coupled-mode method presented in [15].

2. Theoretical model

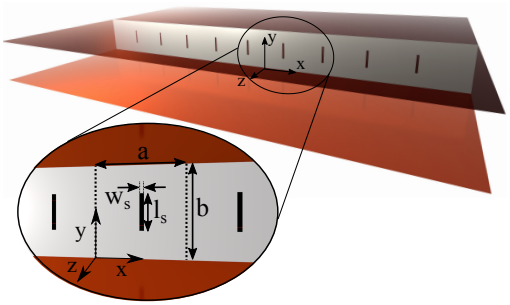

Fig. 1. Perspective view of a parallel plate waveguide. The two plates are connected through a negligible thickness PEC strip perforated with an infinite 1-D periodic array of slots. A zoomed view of the hole array with the definition of the geometry parameters is also shown on the bottom-left of the figure.

Let us consider the problem depicted in Fig. 1, where one pure TE_1^z mode propagating in an infinite PPWG impinges on a negligible thickness conducting strip filling the space between the waveguide plates. The strip, located at $z = 0$, is perforated with a 1-D periodic array of holes. The holes will be assumed to be rectangular slots for the sake of mathematical simplicity, although the physics governing the problem would remain identical if circular holes were to be chosen as in [15]. Both the parallel plates and the strip containing the holes will be assumed to be perfect electric conductors (PECs). In the following, a time-harmonic dependence of the physical quantities of the type $\mathrm{e}^{\mathrm{j}\omega t}$ will be assumed and suppressed throughout. Under these conditions, the complex electric field of the TE_1^z mode incident on the array of slots can be written as [16]

$$\mathbf{E}_1^{\mathrm{PPWG}} = E_0^{\mathrm{PPWG}} \left(\mathrm{e}^{-\mathrm{j}\mathbf{k}_{1,-}} - \mathrm{e}^{-\mathrm{j}\mathbf{k}_{1,+}} \right) \hat{\mathbf{x}} \tag{1}$$

where $\mathbf{k}_{1,-} = -(\pi/b)\hat{\mathbf{y}} + \sqrt{k_0^2 - (\pi/b)^2}\hat{\mathbf{z}}$ and $\mathbf{k}_{1,+} = +(\pi/b)\hat{\mathbf{y}} + \sqrt{k_0^2 - (\pi/b)^2}\hat{\mathbf{z}}$ ($k_0 = \omega\sqrt{\mu_0\epsilon_0} = 2\pi/\lambda_0$, λ_0 being the free space wavelength). Equation (1) indicates that the TE_1^z mode of the PPWG can be seen as the sum of two plane waves, the first propagating with wavenumber vector $\mathbf{k}_{1,-}$ along the direction given by the angular spherical coordinates $(\phi_{\mathrm{inc}}^-, \theta_{\mathrm{inc}}^-) = (3\pi/2, \theta_0)$, and the second propagating with wavenumber vector $\mathbf{k}_{1,+}$ along the direction given by the angular spherical coordinates $(\phi_{\mathrm{inc}}^+, \theta_{\mathrm{inc}}^+) = (\pi/2, \theta_0)$, where

$$\theta_0 = \arctan\left(\frac{\pi}{\sqrt{k_0^2 b^2 - \pi^2}} \right) \tag{2}$$

Imagine each of the two aforementioned plane waves separately propagates in free space and is obliquely incident on a 2-D periodic array of rectangular slots perforated in a PEC screen at $z = 0$ shown in Fig. 2, where the unit cell is exactly equal to that of the 1-D periodic structure of Fig. 1. If we superpose these two waves in the way shown in (1), the resulting wave will fulfill the electric wall (EW) boundary conditions imposed by the PPWG of Fig. 1 at $y = 0$ and $y = b$. This means the problem of the transmission of the TE_1^z mode through the 1-D array of holes can be viewed as the superposition of two problems of transmission of plane waves propagating in free space which are obliquely incident on a 2-D periodic array of holes in a conducting screen, and the superposition principle can be invoked.

Now let us concentrate on the problem of a plane wave obliquely incident on the 2-D array of rectangular slots in a PEC screen that is shown in Fig. 2. Let us assume that the propagation

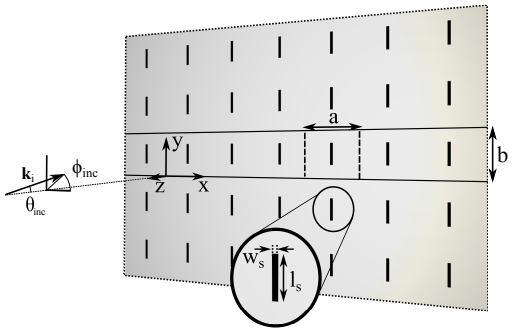

Fig. 2. Perspective view of part of the two dimensional periodic array of holes perforated into a negligible thickness PEC screen. The array is illuminated by an obliquely incident plane wave along the direction given by the spherical angular coordinates $(\phi_{inc}, \theta_{inc})$. A zoomed view of the hole array with the definition of the geometry parameters is also shown.

direction of the plane wave is given by the angular spherical coordinates $(\phi_{\text{inc}}, \theta_{\text{inc}})$ shown in Fig. 2. The complex electric field of this wave can be written as

$$\mathbf{E}_i = E_0 \mathrm{e}^{\mathrm{j}(k_{x0}x + k_{y0}y + k_{z0}z)} \hat{\mathbf{u}} = E_0 \mathrm{e}^{-\mathrm{j}\mathbf{k}_i \cdot \mathbf{r}} \hat{\mathbf{u}} \tag{3}$$

where $k_{x0} = -k_0 \sin\theta_{\text{inc}} \cos\phi_{\text{inc}}$, $k_{y0} = -k_0 \sin\theta_{\text{inc}} \sin\phi_{\text{inc}}$, $k_{z0} = -k_0 \cos\theta_{\text{inc}}$, and $\hat{\mathbf{u}}$ is a unit vector such that $\hat{\mathbf{u}} \cdot \mathbf{k}_i = 0$.

In accordance with the derivations shown in [17] (only valid for the case of normal incidence), in order to determine the scattered tangential electric field, $\mathbf{E}_t^{\text{sc}}(x, y, z = 0)$, in the rectangular slot $\delta_{00} \equiv \{(a - w)/2 < x < (a + w)/2;\ (b - l)/2 < y < (b + l)/2\}$ of the reference unit cell $C_{00} \equiv \{0 \le x \le a;\ 0 \le y \le b\}$ of the 2-D periodic array of slots shown in Fig. 2, we need to solve the integral equation

$$\mathbf{J}^{\text{as}} + \int_0^a \int_0^b \overline{\mathbf{G}}_M^{\text{per}}(x - x', y - y') \cdot \mathbf{E}_t^{\text{sc}}(x', y', z = 0)\, dx' dy' = \mathbf{0} \qquad (x, y) \in \delta_{00} \tag{4}$$

where $\mathbf{J}^{\text{as}}$ is the surface current density that would be induced by the obliquely incident wave in the PEC screen in the absence of rectangular slots, and $\overline{\mathbf{G}}_M^{\text{per}}(x - x', y - y')$ is the periodic dyadic Green's function given by [18]

$$\overline{\mathbf{G}}_M^{\text{per}}(x, y) = \sum_{m=-\infty}^{+\infty} \sum_{n=-\infty}^{+\infty} \overline{\mathbf{G}}_M(x - ma, y - nb)\, \mathrm{e}^{\mathrm{j}(k_{x0}ma + k_{y0}nb)}. \tag{5}$$

In Equation (5), $\overline{\mathbf{G}}_M(x, y)$ stands for the dyadic Green's function defined by

$$\overline{\mathbf{G}}_M(x, y) = \begin{pmatrix} \left(k_0^2 + \frac{\partial^2}{\partial y^2}\right) g(x, y) & -\frac{\partial^2 g(x,y)}{\partial x \partial y} \\ -\frac{\partial^2 g(x,y)}{\partial x \partial y} & \left(k_0^2 + \frac{\partial^2}{\partial x^2}\right) g(x, y) \end{pmatrix} \tag{6}$$

where

$$g(x, y) = -\frac{\mathrm{j}\mathrm{e}^{-\mathrm{j}k_0\sqrt{x^2+y^2}}}{\pi k_0 Z_0 \sqrt{x^2 + y^2}} \tag{7}$$

and where k_0 and Z_0 represent the free space wavenumber and impedance ($Z_0 = \sqrt{\mu_0/\epsilon_0}$) respectively.

In order to solve the integral equation of (4), the unknown quantity $\mathbf{E}_t^{\mathrm{sc}}(x, y, z = 0)$ is expanded in terms of basis functions as shown below

$$\mathbf{E}_t^{sc}(x, y, z = 0) \approx \sum_{j=1}^{N_b} f_j \mathbf{b}_j(x, y) \qquad (x, y) \in \delta_{00} \tag{8}$$

where $\mathbf{b}_j(x, y)$ $(j = 1, \ldots, N_b)$ are chosen to be Chebyshev polynomials multiplied by the edge behavior expected for each of the two possible polarizations (see [17] for details). When the approximation of (8) is substituted in (4) and the Galerkin's version of the Method of Moments (MoM) [19] is applied, the following system of linear equations is obtained for the unknown coefficients f_j

$$\sum_{j=1}^{N_b} \Gamma_{ij} f_j = C_i \quad (i = 1, \ldots, N_b) \tag{9}$$

The coefficients of the MoM matrix of (9) can be obtained in the Fourier transform domain as [17]

$$\Gamma_{ij} = ab \sum_{m,n=-\infty}^{\infty} \widetilde{\mathbf{b}}_i^*(k_{xm}, k_{yn}) \cdot \left[\widetilde{\overline{\mathbf{G}}}_M(k_x = k_{xm}, k_y = k_{yn}) \cdot \widetilde{\mathbf{b}}_j(k_{xm}, k_{yn}) \right] \tag{10}$$

where $\widetilde{\mathbf{b}}_j(k_{xm}, k_{yn})$ $(j = 1, \ldots, N_b)$ are the 2-D discrete Fourier transforms of $\mathbf{b}_j(x, y)$, $k_{xm} = 2\pi m/a + k_{x0}$ and $k_{yn} = 2\pi n/b + k_{y0}$. Also, $\widetilde{\overline{\mathbf{G}}}_M(k_x = k_{xm}, k_y = k_{yn})$ is the 2-D continuous Fourier transform of $\overline{\mathbf{G}}_M(x, y)$ sampled at $k_x = k_{xm}$ and $k_y = k_{yn}$, which is given by

$$\widetilde{\overline{\mathbf{G}}}_M(k_x = k_{xm}, k_y = k_{yn}) = \frac{-2}{k_0 Z_0 \sqrt{k_0^2 - k_{xm}^2 - k_{yn}^2}} \times \begin{pmatrix} k_0^2 - k_{yn}^2 & k_{xm} k_{yn} \\ k_{xm} k_{yn} & k_0^2 - k_{xm}^2 \end{pmatrix} \tag{11}$$

The constant terms C_i $(i = 1, \ldots, N_b)$ of the system of equations (9) can be obtained as

$$\begin{aligned} C_i &= -\left(\int_0^a \int_0^b \mathbf{b}_i(x, y) \mathrm{e}^{-\mathrm{j}(k_{x0}x + k_{y0}y)} \, dxdy \right)^* \cdot \mathbf{J}^{\mathrm{as}} \\ &= -ab \, \widetilde{\mathbf{b}}_i^*(k_{x0}, k_{y0}) \cdot \mathbf{J}^{\mathrm{as}}. \end{aligned} \tag{12}$$

Note that the spectral dyadic Green's function $\widetilde{\overline{\mathbf{G}}}_M(k_x = k_{xm}, k_y = k_{yn})$ has poles at frequencies for which

$$\sqrt{k_0^2 - k_{xm}^2 - k_{yn}^2} = 0 \Rightarrow k_{xm}^2 + k_{yn}^2 = k_0^2 \tag{13}$$

When condition (13) is fulfilled, the elements of $\widetilde{\overline{\mathbf{G}}}_M(k_x = k_{xm}, k_y = k_{yn})$ tend to infinity, the MoM matrix entries Γ_{ij} usually tend to infinity and the unknown coefficients f_j tend to zero to keep C_i bounded in (9). As a consequence of this, $\mathbf{E}_t^{sc}(x, y, z = 0)$ becomes zero in (8), which means the tangential electric field in the holes of the 2-D array vanishes, i.e., the PEC screen with holes behaves as a solid PEC and reflects all the incoming power, which is the origin of a Wood's anomaly. Therefore, Equation (13) provides the condition for Wood's anomalies and marks the onset of the $m - n$-th diffracted mode (also called $m - n$-th grating lobe). At

frequencies just below this divergence, the fields on the slot are largely enhanced, providing a mechanism for the appearance of EOT peaks. This has also been explained in terms of circuit theory reported in [14], showing that an EOT peak always appears at a frequency slightly lower than a Wood's anomaly owing to impedance matching provided by a resonance created by a frequency dependent capacitance that becomes singular at the Wood's anomaly. So, a Wood anomaly always presents an associated EOT peak at slightly lower frequencies.

3. Results and discussion

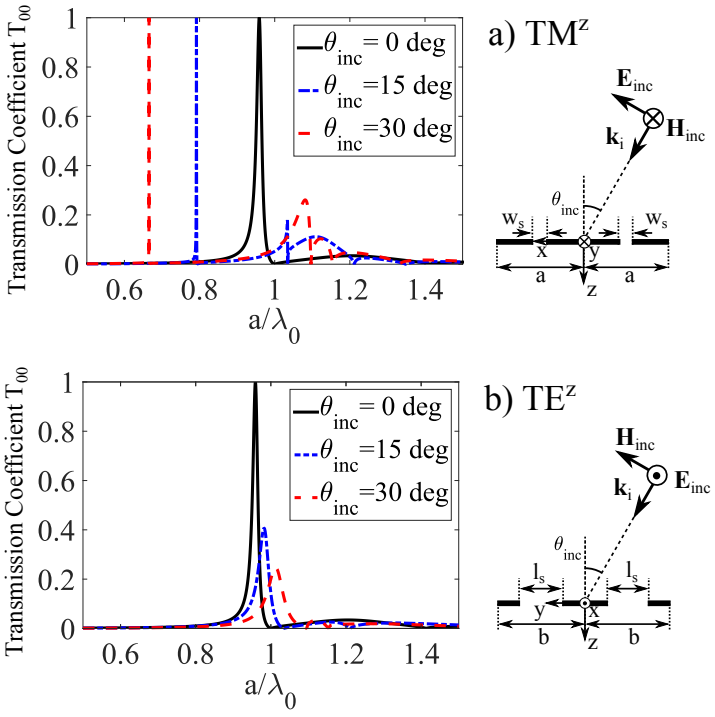

Fig. 3. Transmission spectra of a plane wave impinging on a 2-D array of rectangular slots in a PEC screen. Two polarizations TM^z (a) and TE^z (b) are considered, and different angles of incidence (θ_{inc}). In both cases, the direction of the incident electric field is contained in the $x-z$ plane so as to excite the fields in the slots. The dimensions of the unit cell were chosen to be $l_s/a = 0.4$, $w_s/a = 0.05$ and $a = b$.

For a PEC screen with a 2-D array of holes under normal incidence conditions ($\theta_{\text{inc}} = 0$), the first Wood's anomaly is expected to appear at a frequency for which $\lambda_0 = \max(a, b)$. This corresponds to the Wood's anomaly experimentally detected in [15] for a PPWG under TEM excitation since this problem is equivalent to the EOT problem of a 2-D periodic array of holes under normal incidence [17].

However, for the 2-D array of holes of Fig. 2 under oblique incidence, Wood's anomalies and the associated EOT peaks in principle tend to appear at frequencies above and below the frequency for which $\lambda_0 = \max(a, b)$. For example, let us consider the transmission curves shown in Fig. 3(a) for a 2-D periodic array of rectangular slots illuminated by obliquely incident plane waves propagating along different directions given by $(\phi_{\text{inc}} = 0, \theta_{\text{inc}})$ (all the curves in Fig. 3 have been obtained by means of MoM in accordance with Eqns. (4) to (12)). For these particular incidence directions, we would expect Wood's anomalies for the $m = \pm 1, n = 0$ diffracted modes (see (13)) when $a/\lambda_0 = 1/1 \pm \sin\theta_{\text{inc}}$. Also, we would expect Wood's anomalies for

the $m = 0, n = \pm 1$ modes when $b/\lambda_0 = 1/\cos\theta_{\text{inc}}$. When $a = b$, which is the particular case treated in Fig. 3(a), the Wood's anomalies appear for $a/\lambda_0 < 1$ and $a/\lambda_0 > 1$, i.e., above and below the frequency of the Wood anomaly for normal incidence ($a/\lambda_0 = 1$). Note that total transmission does not occur in the EOT peaks associated with the Wood's anomalies for which $a/\lambda_0 > 1$, which is due to the fact that some diffracted modes have already been launched at those frequencies and are capturing part of the energy of the original incident wave. However, Wood's anomalies and EOT peaks may not always appear for oblique incidence at frequencies below the frequency for which $\lambda_0 = \max(a, b)$. In particular, Fig. 3(b) shows the transmission curves of a 2-D periodic array of rectangular slots illuminated by obliquely incident plane waves propagating along different directions given by $(\phi_{\text{inc}} = \pi/2, \theta_{\text{inc}})$. For these particular incidence directions, we should expect Wood's anomalies for the $m = \pm 1, n = 0$ diffracted modes when $a/\lambda_0 = 1/\cos\theta_{\text{inc}}$, and for the $m = 0, n = \pm 1$ diffracted modes when $b/\lambda_0 = 1/1 \pm \sin\theta_{\text{inc}}$.

In the case shown in Fig. 3(b) where $a = b$, the Wood anomalies and EOT peaks for the $m = \pm 1, n = 0$ modes appear when $a/\lambda_0 > 1$, but those for the $m = 0, n = \pm 1$ modes do not appear when $a/\lambda_0 < 1$. The explanation for this latter behavior is hidden in Eqns. (10) and (11). Under the conditions studied in Fig. 3(b), it turns out that $k_{x0} = 0$. This means that when Eqn. (13) is fulfilled for the $m = 0, n = \pm 1$ modes, there is a zero-pole cancellation in all the elements of the matrix $\widetilde{\widetilde{\mathbf{G}}}_M(k_x = k_{x0}, k_y = k_{y,\pm 1})$ except for the $y - y$ element. Also, under the illumination conditions studied in Fig. 3(b), the functions $\mathbf{b}_j(x, y) \cdot \hat{\mathbf{y}}$ are odd functions of x since the planes $x = ma + a/2$ ($m = \ldots, -1, 0, 1, \ldots$) of the 2-D periodic array are all EWs [17]. As a consequence of this, it turns out that $\widetilde{\mathbf{b}}_j(k_{x0} = 0, k_{y,\pm 1}) \cdot \hat{\mathbf{y}} = 0$. So, when $\widetilde{\widetilde{\mathbf{G}}}_M(k_x = k_{x0}, k_y = k_{y,\pm 1})$ and $\widetilde{\mathbf{b}}_j(k_{x0} = 0, k_{y,\pm 1})$ are both substituted in (10), there is an additional zero-pole cancellation that prevents Γ_{ij} from being infinite when $m = 0, n = \pm 1$ and condition (13) is fulfilled. Note that total transmission does not occur in the EOT peaks associated with the $m = \pm 1, n = 0$ modes in Fig. 3(b) when $\theta_{\text{inc}} \neq 0$, which indicates that the $m = 0, n = \pm 1$ diffracted modes have been launched, even though the Wood's anomaly and EOT peaks for these modes have not appeared.

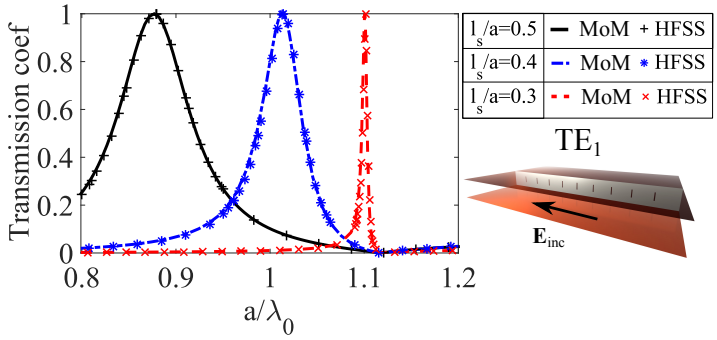

Fig. 4. Transmission spectra obtained when the TE_1 mode of the PPWG of Fig. 1 impinges on the 1-D array of rectangular slots. Our results (MoM) are compared with HFSS results. The dimensions of the unit cell were chosen to be $w_s/a = 0.05$ and $a = b$.

The MoM formulation of (4) to (12) and the superposition principle have both been used to compute the transmission through the 1-D array of rectangular slots of Fig. 1 under TE_1^z mode excitation. The results are plotted in Fig. 4. For validation purposes, our MoM results have been compared with results obtained by the commercial software HFSS, and excellent agreement has been found. It should be pointed out that our in-house software is about 225 times faster than HFSS for the generation of Fig. 3, which justifies the efforts carried out to develop in-house software in addition to the physical insight provided for the understanding of the Wood's anomaly phenomena.

Taking into account the Wood's anomalies detected in Fig. 3(b) for the diffracted modes $m = \pm 1, n = 0$, we have inserted these two values of m and n in (13) plus the incidence angle values ($\phi_{\text{inc}} = \pi/2 | 3\pi/2, \theta_{\text{inc}} = \theta_0$) (where θ_0 is defined in (2)) for the TE_1^z mode in the PPWG, and we have found that a Wood's anomaly and the associated EOT peak is to be expected when $a/\lambda_0 = b/\lambda_0 = \sqrt{5}/2 > 1$ ($a = b$ has been assumed in Fig. 4). This exactly coincides with the results obtained in Fig. 4, and it can be verified that this frequency estimation for the Wood's anomaly roughly matches those experimentally obtained by Reichel et al. [15] under TE_1^z mode excitation.

There is another way to explain the appearance of the Wood's anomaly for $a/\lambda_0 = b/\lambda_0 = \sqrt{5}/2 > 1$, which is based on the fact that the planes $x = ma$ and $x = ma + a/2$ ($m = \ldots, -1, 0, 1, \ldots$) act as EWs and the plane $y = b/2$ acts as a magnetic wall (MW) in Fig. 1 under TE_1^z mode excitation. This means the periodic unit cell acts as an equivalent rectangular waveguide excited by a TE_{01} mode. The symmetry conditions imposed by the EWs and the MWs mean that the first higher order TM mode that can be excited in this equivalent waveguide is a TM_{21} mode. Since TM modes in rectangular waveguides are precisely those which give rise to Wood's anomalies and EOT peaks [12, 14], it is clear that the first Wood's anomaly of the PPWG under TE_1^z mode excitation will show up at the cutoff frequency of the TM_{21} mode, which occurs for $a/\lambda_0 = b/\lambda_0 = \sqrt{5}/2$ when $a = b$. This is in agreement with previous studies of EOT in hollow metal waveguides [12]. When $a/\lambda_0 = b/\lambda_0 > \sqrt{5}/2$, a combination of TE_1 and TM_1 modes will be excited in the PPWG propagating at oblique angles from the z direction since TM_{21} modes cannot propagate in a PPWG.

4. Conclusion

In summary, we have presented a theory based on the application of the Method of Moments that explains why the EOT peaks of PPWG with 1-D periodic arrays of symmetric holes under TE_1^z mode excitation appear at frequencies higher than those found for TEM mode excitation. The theory indicates that EOT peaks for TE_1^z excitation should also be expected at frequencies lower than those of TEM mode excitation, but they do not appear because of the symmetry of the holes. The symmetry plane perpendicular to the x axis eliminates the divergent response of the fields on the first onset of diffraction, therefore finding the first peak associated to extraordinary transmission at higher frequencies than at normal incidence.

Funding

Engineering and Physical Sciences Research Council (EPSRC) (EP/L015331/1) and "Junta de Andalucía" (P12-TIC-1435).

Acknowledgement

All data created during this research are openly available from the University of Exeter's institutional repository at https://ore.exeter.ac.uk/.